AIP | Applied Physics Letters

Room-temperature ferromagnetism in (Mn, N)-codoped ZnO thin films prepared by reactive magnetron cosputtering

H. Y. Xu, Y. C. Liu, C. S. Xu, Y. X. Liu, C. L. Shao et al.

Citation: Appl. Phys. Lett. **88**, 242502 (2006); doi: 10.1063/1.2213929
View online: http://dx.doi.org/10.1063/1.2213929
View Table of Contents: http://apl.aip.org/resource/1/APPLAB/v88/i24
Published by the American Institute of Physics.

Room-temperature ferromagnetism in (Mn, N)-codoped ZnO thin films prepared by reactive magnetron cosputtering

H. Y. Xu
Center for Advanced Optoelectronic Functional Material Research, Northeast Normal University, Changchun 130024, China and Key Laboratory of Excited State Processes, Changchun Institute of Optics, Fine Mechanics and Physics, Chinese Academy of Science, Changchun 130033, China

Y. C. Liu,[a] C. S. Xu, Y. X. Liu, and C. L. Shao
Center for Advanced Optoelectronic Functional Material Research, Northeast Normal University, Changchun 130024, China

R. Mu
Department of Physics, Fisk University, Nashville, Tennessee 37208

(Received 8 December 2005; accepted 6 May 2006; published online 12 June 2006)

(Mn, N)-codoped ZnO films were grown on fused silica substrates by reactive magnetron cosputtering. X-ray diffraction measurements reveal that the films have the single-phase wurtzite structure with *c*-axis preferred orientation. X-ray photoelectron spectroscopy studies indicate the incorporation of both divalent Mn^{2+} and trivalent N^{3-} ions into ZnO lattice. Acceptor doping with nitrogen partly compensates the "native donors," which results in a low electron concentration of 3.16×10^{16} cm^{-3} though *p*-type conductivity is not achieved. (Mn, N)-codoped ZnO films show significant ferromagnetism with Curie temperature above 300 K. The mechanism of ferromagnetic coupling in codoped ZnO is discussed based on a bound magnetic polaron model. © *2006 American Institute of Physics*. [DOI: 10.1063/1.2213929]

ZnO material has been extensively studied in recent years for various optoelectronic applications, such as, ultraviolet lasers,[1,2] light-emitting diodes,[3,4] thin film transistors,[5] transparent conductors,[6] etc. Currently, ZnO-based diluted magnetic semiconductors (DMSs), which involve charge and spin degrees of freedom in a single substance, are attracting much more attention due to their potential applications in "spintronic" devices. DMS ferromagnetism above room temperature is highly desirable for many practical applications. Several theoretical calculations[7–9] have predicted that the *p*-type Mn-doped ZnO (ZnO:Mn) would show ferromagnetism with Curie temperature (T_C) well above room temperature. Motivated by these predictions, many efforts have been made to investigate ZnO:Mn systems. However, the reported experimental results have been inconsistent and sometimes controversial. Some groups have reported ferromagnetism but with different T_C in *p*-type and even *n*-type ZnO:Mn systems,[10–17] whereas others have only observed paramagnetic or antiferromagnetic behaviors.[18–21] Thus, more research is needed to understand the underlying causes of the inconsistency.

A recent theoretical study by Wang *et al.* has predicted the hole-mediated ferromagnetism in (Mn, N)-codoped ZnO thin films [ZnO:(Mn, N)].[9] In their model, nitrogen is employed as an ideal *p*-type dopant. However, codoping of ZnO with Mn and N is not easy to achieve experimentally. Reactive magnetron sputtering is a flexible and effective method to deposit doped films. In our previous work, for example, this technique has been used to prepare N-doped ZnO films with various N concentrations.[22] In this letter, we report the fabrication of ZnO:(Mn, N) films using reactive magnetron cosputtering, and demonstrate their room-temperature ferromagnetism.

ZnO:(Mn, N) thin films were grown on fused silica substrates by radio-frequency (rf) reactive magnetron cosputtering. The sputtering target consisted of a high-purity Zn disk (100 mm in diameter) and some smaller and thin Mn pieces (~8 mm in diameter) placed equidistantly on Zn disk. The composition ratio of Zn/Mn in the sputtered films can be adjusted by varying the number of Mn pieces. In this experiment, we have controlled the Mn-doping level at ~5 at. %. The sputtering chamber was first evacuated to a base pressure below 3×10^{-4} Pa with a turbo molecular pump. And then, ultrapure Ar, O_2, and N_2 mixed gases were introduced into the chamber with flow rates of 160, 40, and 20 SCCM (SCCM denotes cubic centimeter per minute at STP), respectively. During film deposition, the substrate temperature, rf power, and sputtering pressure were kept at 300 °C, 200 W, and 1.0 Pa, respectively. The above chosen parameters have been determined as the optimal growth conditions. For a reference purpose, a Mn-only doped ZnO film was also prepared under almost the same conditions but without the introduction of N_2 plasma.

The structure and composition of the deposited films were characterized by x-ray diffraction (XRD) and high resolution x-ray photoelectron spectroscopy (XPS). Before XPS measurements, the surface layer of the sample was removed with Ar^+ bombardment to reduce the possible surface contamination. Electrical properties of the films were investigated by van der Pauw Hall measurements (Model 7707, LakeShore Co.). Magnetic measurements were performed with a superconducting quantum interference device (SQUID) magnetometer (Quantum Design, MPMS-XL) in the temperature range from 5 to 300 K and fields of up to 6 kOe.

[a]Author to whom correspondence should be addressed; electronic mail: ycliu@nenu.edu.cn

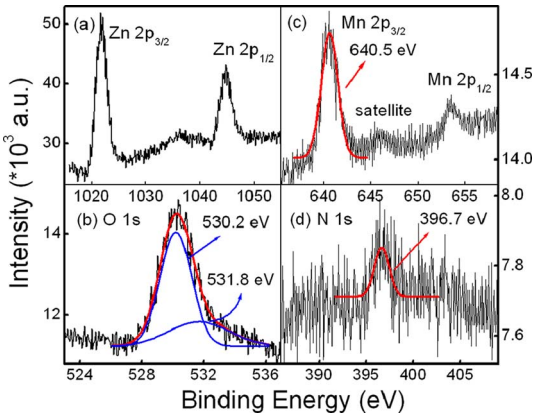

FIG. 1. (Color online) XPS spectra of (a) Zn 2*p*, (b) O 1*s*, (c) Mn 2*p*, and (d) N 1*s* core levels for $Zn_{.95}Mn_{.05}O_{.93}N_{.07}$ film.

Figure 1 shows XPS spectra of ZnO:(Mn, N) film. The core level peaks of Zn 2*p*, O 1*s*, Mn 2*p*, and N 1*s* were observed. The binding energy of Zn $2p_{3/2}$ is located at 1021.7 eV, suggesting a single component of Zn^{2+} ions. The O 1*s* peak is broad and asymmetric. It can be well fitted by two Gaussian curves, as shown in Fig. 2(b). The stronger peak at 530.2 eV may be attributed to O^{2-} ions in Zn–O and Mn–O bonds, while another at 531.8 eV is usually associated with the loosely bound oxygen (e.g., adsorbed O_2, –OH) chemisorbed on the surface and/or grain boundary of polycrystalline film.[22,23] The incorporation of both Mn and N is clearly demonstrated by the core level spectra of Mn 2*p* and N 1*s*. The Mn $2p_{3/2}$ peak appears at 640.5 eV and has a narrow linewidth of 1.8 eV. No XPS signals from metallic Mn (637.7 eV) and Mn^{4+} ions (642.4 eV) were detected. These results indicate that the doped Mn ions are in divalent states.[24] It is also noted that the Mn^{2+} $2p_{3/2}$ main peak has the satellite structure on the higher energy side separated by ~6 eV. This observation is also consistent with other reports.[24,25] In the N 1*s* spectrum, a weak peak at 396.7 eV was detected. This peak is usually attributed to the Zn–N bond formation as a result of N ions substitution.[22,26] The quantitative analysis indicates that the concentrations of Mn and N in codoped film are 5.0 and 6.6 at. % ($Zn_{.95}Mn_{.05}O_{.93}N_{.07}$), respectively. In the case of Mn-only doped ZnO, the Mn concentration is estimated to be ~5.4 at. % ($Zn_{.95}Mn_{.05}O$).

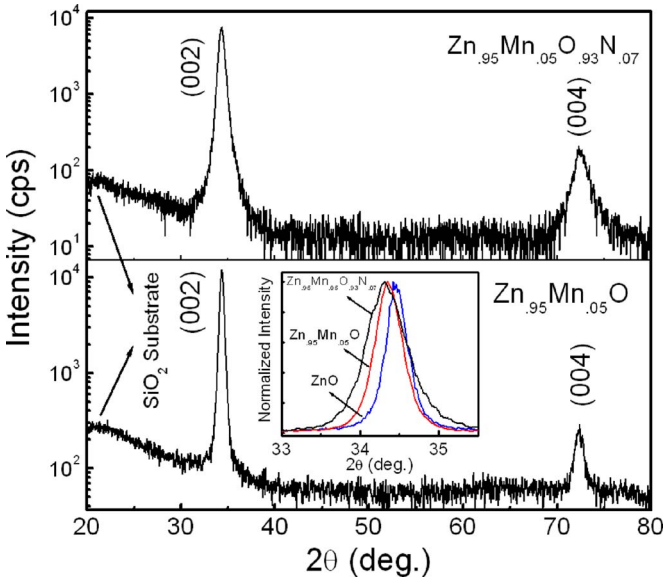

FIG. 2. (Color online) Semilogarithmic XRD spectra of $Zn_{.95}Mn_{.05}O_{.93}N_{.07}$ and $Zn_{.95}Mn_{.05}O$ films.

TABLE I. Electrical parameters of $Zn_{0.95}Mn_{0.05}O_{0.93}N_{0.07}$ and $Zn_{0.95}Mn_{0.05}O$ films.

Samples	Type	ρ (Ω cm)	μ ($cm^2\ V^{-1}\ s^{-1}$)	N (cm^{-3})
$Zn_{0.95}Mn_{0.05}O$	*e*	6.50	0.62	1.55×10^{18}
$Zn_{0.95}Mn_{0.05}O_{0.93}N_{0.07}$	*e*	5.64×10^{2}	0.35	3.16×10^{16}

Figure 2 shows the semilogarithmic plots of XRD patterns for $Zn_{.95}Mn_{.05}O_{.93}N_{.07}$ and $Zn_{.95}Mn_{.05}O$ films. Except for ZnO (002) and (004) orientations, no extra diffraction peaks from Mn-related secondary phases or impurities were observed. This indicates that both films are single phase and have hexagonal wurtzite structure with *c*-axis preferred orientation. It is known that the ionic radii of the substitutional Mn^{2+} (80 pm) and N^{3-} (132 pm) are larger than those of Zn^{2+} (74 pm) and O^{2-} (124 pm). Thus, codoping with Mn and N causes a slight shift of XRD peaks toward the lower diffraction angle, as shown in the inset of Fig. 2. Correspondingly, the *c*-axis lattice constant increases from 5.201 Å for undoped ZnO to 5.222 Å for $Zn_{.95}Mn_{.05}O_{.93}N_{.07}$. Moreover, for doped films, the linewidths of XRD peaks are considerably broadened due to microscopic structural disorder and lattice strain induced by Mn and N ions' substitution.[14,27] The lattice disorder in ZnO:Mn has also been reported and discussed in our previous Raman scattering studies.[28]

The resistivity and Hall measurements of the doped ZnO films were performed and the experimental data were listed in Table I. The undoped ZnO film usually exhibits *n*-type conductivity due to the presence of oxygen vacancies and zinc interstitials. The substitution of divalent Mn^{2+} ions would not introduce additional charge carriers. Thus, $Zn_{.95}Mn_{.05}O$ film shows a high electron concentration of 1.55×10^{18} cm^{-3}. On the other hand, the substitution of N^{3-} ions for O^{2-} ions may provide more hole carriers, but they are largely compensated by the "native donors" present in ZnO films. Thus, we were unable to achieve the *p*-type conductivity in the present effort. However, as a result of N-acceptor doping, the effective electron concentration in $Zn_{.95}Mn_{.05}O_{.93}N_{.07}$ film decreases significantly to 3.16×10^{16} cm^{-3}.

The magnetization of both films was measured as functions of magnetic field (*M-H*) and temperature (*M-T*), as shown in Fig. 3. The diamagnetic contribution from silica substrate has been subtracted from the raw data. The *M-H* curve of $Zn_{.95}Mn_{.05}O$ shows a nearly linear paramagnetic behavior at 300 K, suggesting the absence of interactions among the Mn moments. In contrast, the *M-H* curve of $Zn_{.95}Mn_{.05}O_{.93}N_{.07}$ film at 300 K exhibits a clear hysteresis loop with a coercive field of 80 Oe and a saturation magnetization of $0.35\mu_B$/Mn, revealing a room-temperature ferromagnetic characteristic. The inset of Fig. 3 shows the *M-T* curve of the codoped film. The magnetization decreases slightly with increasing temperature. However, the transition from ferromagnetic to paramagnetic state does not occur in the temperature range of 5–300 K, indicating a T_C in excess of at least 300 K. It is also noted that the measured saturation magnetization of $0.35\mu_B$/Mn is much smaller than the theo-

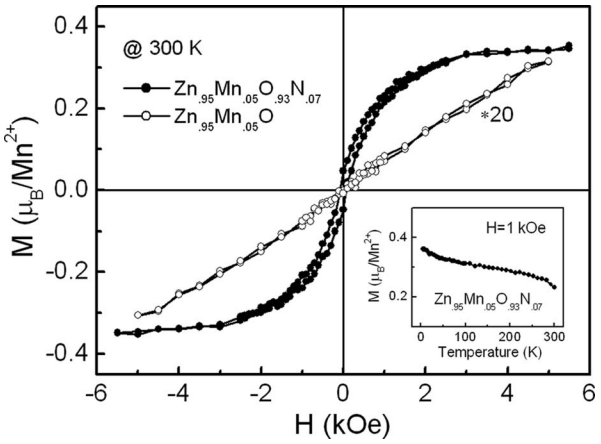

FIG. 3. (Color online) Room-temperature M-H curves of $Zn_{.95}Mn_{.05}O_{.93}N_{.07}$ and $Zn_{.95}Mn_{.05}O$ films; insert: M-T curve of codoped film under applied magnetic field of 1 kOe.

retical value of $\sim 5\mu_B$/Mn for a free Mn^{2+} ion. This phenomenon is common in DMSs, which usually is ascribed to antiferromagnetic superexchange interactions between neighboring Mn^{2+} ions.[13,28]

When assigning the origin of ferromagnetism, one should carefully consider the possibility of material phase segregation even though no secondary phases have been detected in XRD and XPS measurements. The possible "impurities," including Mn metal and almost all the Mn-based oxides, are antiferromagnetic. An exception is ferromagnetic Mn_3O_4 with T_C of ~ 42 K. However, this phase could not be responsible for 300 K ferromagnetism. Therefore, we expect that the room-temperature ferromagnetism observed in our experiment originates from $Zn_{.95}Mn_{.05}O_{.93}N_{.07}$ structure.

The experimental observations have demonstrated that N doping plays a crucial role in the activation of ferromagnetism. Our results are consistent with the reports by Gamelin and co-workers.[11,12] In their studies, high-T_C ferromagnetism in ZnO:Mn was activated by amine surface capping, though the material was not globally p type. They have attributed ferromagnetic mechanism to the formation of bound magnetic polaron (BMP).[11,17,29,30] A similar situation may also be present in our ZnO:(Mn, N) system. Though weakly n-type conductivity has been determined by Hall measurements, it is still possible that some uncompensated or localized holes exist in our sputtered ZnO:(Mn, N) polycrystalline film, because N acceptor-related emission has been observed in our previous photoluminescence studies of the sputtered ZnO:N films.[22] Exchange interactions between one localized hole and many surrounding Mn^{2+} ions align all the Mn^{2+} spins around the hole localization center, forming a BMP.[29,30] The overlapping of neighboring BMPs can result in the long-range Mn^{2+}–Mn^{2+} ferromagnetic coupling in ZnO:(Mn, N). However, until now, ferromagnetic mechanisms of DMS are still controversial. More work is needed to illustrate the fundamental physical processes.

In summary, the single-phase ZnO:(Mn, N) films with a c-axis oriented wurtzite structure were grown on fused silica substrates by reactive magnetron cosputtering. Room-temperature ferromagnetism in ZnO:Mn film is activated by codoping with N. The experimental results not only have fundamental importance, but also provide an effective method to achieve high-T_C ferromagnetism in ZnO-based DMSs. Further work is in progress to investigate the effects of Mn and N concentrations on the magnetic properties of ZnO:(Mn, N) films.

This work is supported by Cultivation Fund of the Key Scientific and Technical Innovation Project (No. 704017), Ministry of Education of China; National Natural Science Foundation of China (Grant Nos. 60376009 and 60576040), and Science Foundation for Young Teachers of Northeast Normal University (Grant No. 20060201). One of the authors (R.M.) would like to acknowledge the supports from DOD, ARO, NSF, and DOE/NREL of United States.

[1] H. Cao, J. Y. Xu, E. W. Seeling, and R. P. H. Chang, Appl. Phys. Lett. **76**, 2997 (2000); Phys. Rev. Lett. **84**, 5584 (2000).
[2] Z. K. Tang, G. K. L. Wong, P. Yu, M. Kawasaki, A. Ohtomo, H. Koinuma, and Y. Segawa, Appl. Phys. Lett. **72**, 3270 (1998).
[3] A. Tsukazaki, A. Ohotmo, T. Onuma, M. Ohtani, T. Makino, M. Sumiya, K. Ohtani, Shigefusa F. Chichibu, S. Fuke, Y. Segawa, H. Ohno, H. Koinuma, and M. Kawasaki, Nat. Mater. **4**, 42 (2005).
[4] H. Y. Xu, Y. C. Liu, Y. X. Liu, C. S. Xu, C. L. Shao, and R. Mu, Appl. Phys. B: Lasers Opt. **80**, 871 (2005).
[5] P. F. Carcia, R. S. McLean, M. H. Reilly, and G. Nunes, Jr., Appl. Phys. Lett. **82**, 1117 (2003).
[6] H. Y. Xu, Y. C. Liu, R. Mu, C. L. Shao, Y. M. Lu, D. Z. Shen, and X. W. Fan, Appl. Phys. Lett. **86**, 123107 (2005).
[7] T. Dietl, H. Ohno, F. Matsukura, J. Cubert, and D. Ferrand, Science **287**, 1019 (2000).
[8] K. Sato and H. Katayama-Yoshida, Physica B **308–310**, 904 (2001); Physica E (Amsterdam) **10**, 251 (2001).
[9] Q. Wang, Q. Sun, P. Jena, and Y. Kawazoe, Phys. Rev. B **70**, 052408 (2004).
[10] S.-W. Lim, M.-C. Jeong, M.-H. Ham, and J.-M. Myoung, Jpn. J. Appl. Phys., Part 2 **43**, L280 (2004).
[11] Kevin R. Kittilstved, and Daniel R. Gamelin, J. Am. Chem. Soc. **127**, 5292 (2005).
[12] Kevin R. Kittilstved, Nick S. Norberg, and Daniel R. Gamelin Phys. Rev. Lett. **94**, 147209 (2005).
[13] P. Sharma, A. Gupta, K. V. Rao, F. J. Owens, R. Sharma, R. Ahuja, J. M. Osorio Guillen, B. Johansson, and G. A. Gehring, Nat. Mater. **2**, 673 (2003).
[14] S. W. Jung, S. J. An, G. Yi, C. U. Jung, S. Lee, and S. Cho, Appl. Phys. Lett. **80**, 4561 (2002).
[15] D. P. Norton, S. J. Pearton, A. F. Hebard, N. Theodoropoulou, L. A. Boatner, and R. G. Wilson, Appl. Phys. Lett. **82**, 239 (2003).
[16] Y. W. Heo, M. P. Ivill, K. Ip, D. P. Norton, S. J. Pearton, J. G. Kelly, R. Rairigh, A. F. Hebard, and T. Steiner, Appl. Phys. Lett. **84**, 2292 (2004).
[17] M. Ivill, S. J. Pearton, D. P. Norton, J. Kelly, and A. F. Hebard, J. Appl. Phys. **97**, 053904 (2005).
[18] X. M. Cheng and C. L. Chien, J. Appl. Phys. **93**, 7876 (2003).
[19] A. Tiwari, C. Jin, A. Kivt, D. Kumar, J. F. Muth, and J. Narayan, Solid State Commun. **121**, 371 (2002).
[20] J. Luo, J. K. Liang, Q. L. Liu, F. S. Liu, Y. Zhang, B. J. Sun, and G. H. Rao, J. Appl. Phys. **97**, 086106 (2005).
[21] T. Fukumura, Zhengwu Jin, M. Kawasaki, T. Shono, T. Hasegawa, S. Koshihara, and H. Koinuma, Appl. Phys. Lett. **78**, 958 (2001).
[22] J. G. Ma, Y. C. Liu, R. Mu, J. Y. Zhang, Y. M. Lu, D. Z. Shen, and X. W. Fan, J. Vac. Sci. Technol. B **22**, 94 (2004).
[23] M. Chen, X. Wang, Y. H. Yu, Z. L. Pei, X. D. Bai, C. Sun, R. F. Huang, and L. S. Wen, Appl. Surf. Sci. **158**, 134 (2000).
[24] Z. B. Gu, C. S. Yuan, M. H. Lu, J. Wang, D. Wu, S. T. Zhang, S. N. Zhu, Y. Y. Zhu, and Y. F. Chen, J. Appl. Phys. **98**, 053908 (2005).
[25] T. Mizokawa, T. Nambu, A. Fujimori, T. Fukumura, and M. Kawasaki, Phys. Rev. B **65**, 085209 (2002).
[26] Craig L. Perkins, S. Lee, X. Li, Sally E. Asher, and Timothy J. Coutts, J. Appl. Phys. **97**, 034907 (2005).
[27] C. Liu, F. Yun, B. Xiao, S.-J. Cho, Y. T. Moon, H. Morkoç, Morad Abouzaid, R. Ruterana, K. M. Yu, and W. Walukiewicz, J. Appl. Phys. **97**, 126107 (2005).
[28] H. Y. Xu, Y. C. Liu, C. S. Xu, Y. X. Liu, C. L. Shao, and R. Mu, J. Chem. Phys. **124**, 074707 (2006).
[29] A. Kaminski and S. Das Sarma, Phys. Rev. Lett. **88**, 247202 (2002).
[30] C. Liu, F. Yun, and H. Morkoç, J. Mater. Sci.: Mater. Electron. **16**, 555 (2005).